Simulation of the evolution of runaway electrons in tokamaks with pellet suppression and instability effects

Don Spong, Diego del-Castillo Negrete, Leopoldo Carbajal Gomez, Larry Baylor
Oak Ridge National Laboratory

PPPL Workshop: Theory and Simulation of Disruptions

July 17-19, 2017 Princeton Plasma Physics Laboratory, Princeton, NJ

Work supported by U.S. Department of Energy, Office of Science Contracts DE-AC05-00OR22725, DE-SC0013804, and under the U.S. DOE SciDAC GSEP Center. This research used resources of the Oak Ridge Leadership Computing Facility at the Oak Ridge National Laboratory, which is supported by the Office of Science of the U.S. Department of Energy under Contract No. DE-AC05-00OR22725

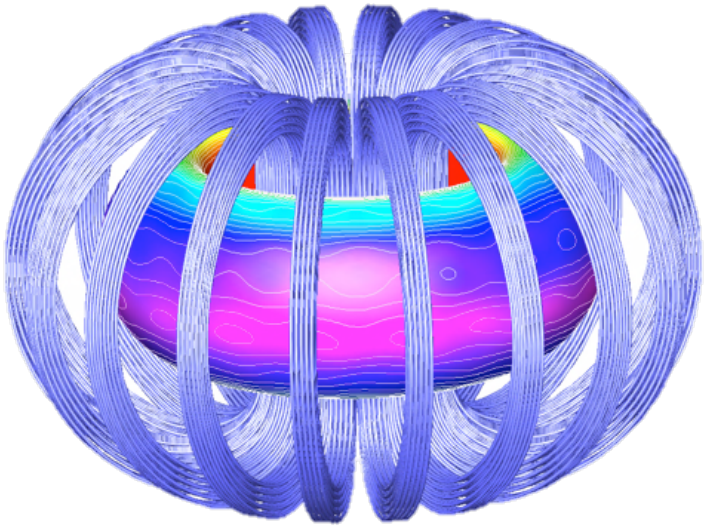

The control and modeling of runaways

- **Formation: prediction of runaway source**
  - Disruption prediction/modeling
  - Runaway generation and acceleration
  - Collisional and synchrotron losses
  - Avalanche effects
- **Suppression: mitigation strategy**
  - Runaway interaction with MGI/pellet ablation cloud
  - Collisional effects, impurities, screening, synchrotron losses, etc.
  - Interaction with electromagnetic waves, MHD, field line stochasticity
- **The KORC-GC model can treat both limits**
  - For this talk we focus on the mitigation strategy topic

Runaway electron issues for mitigation

Runaway sources

- Ohmic E_{tor}
- **Current quench generation**
- Knock-on runaways

Confinement

- 100's of MeV in ITER
- Magnetic islands, 3D perturbation fields, macro equilibrium
- Heat loads on plasma facing components

Mitigation

- disruption avoidance
- **shattered pellets (ORNL)**
- **massive gas injection**

Relativistic trapped/passing orbits in ITER using ORNL MC code + 3D VMEC with field ripple and TBM perturbations

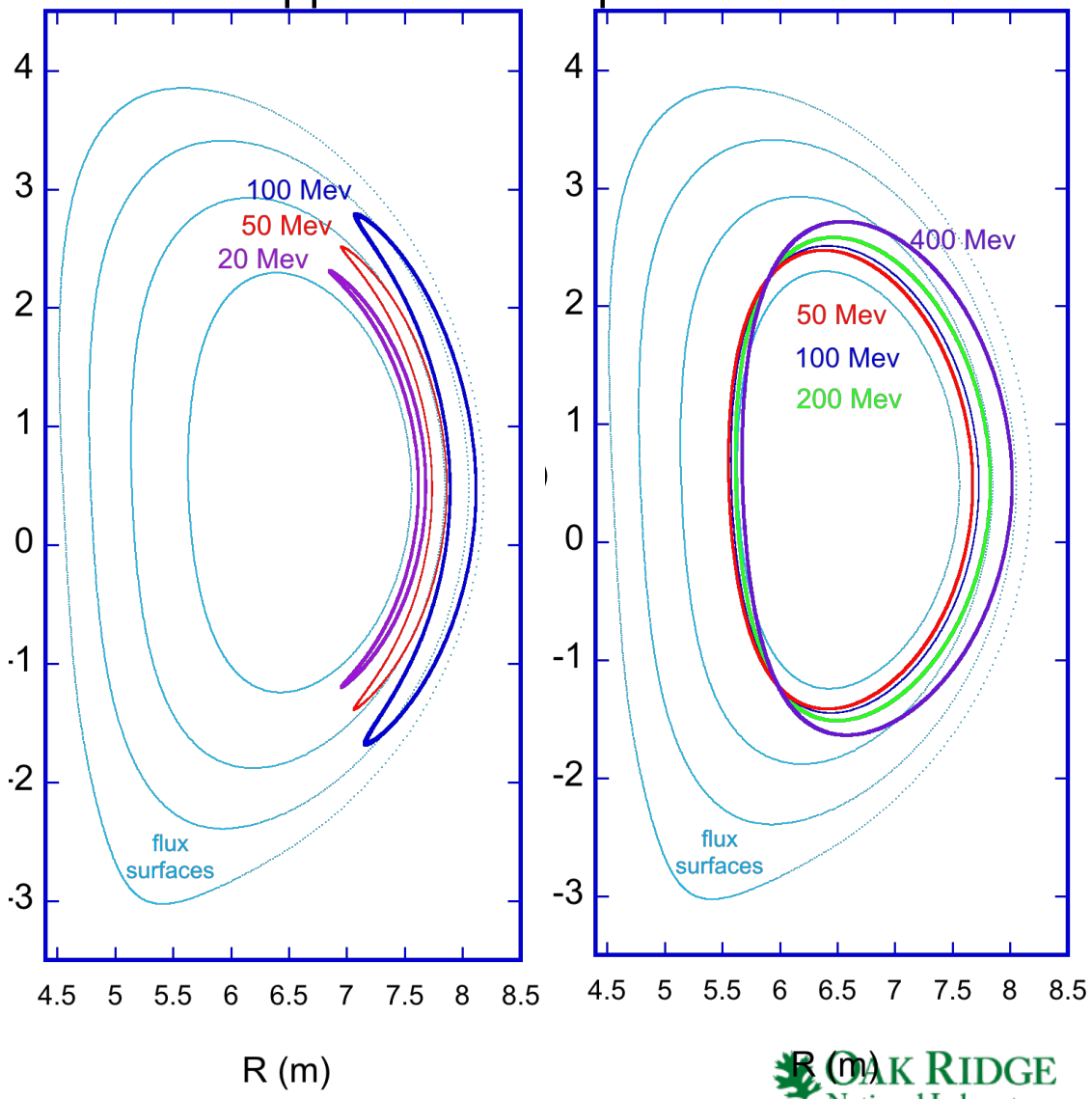

KORC-GC runaway Monte Carlo model

- Guiding-center approximation
  - Requires small gyro-radius, small change in B during parallel motion over a gyro-period
  - Faster integration speed good for parameter studies
- Runaways followed through 5D phase space
  - 3 dimensions + energy, pitch angle
  - Coulomb collisions + recent impurity screening effects of L. Hesslow, O. Embréus, et al., PRL **118**, 255001 (2017).
  - VMEC based – accepts 3D equilibria
- Particle method allows easy treatment of
  - 3D time-evolving pellet clouds
  - Rapidly changing plasma parameters
    - Runaway orbit time step ~ 0.5 nanosecond
  - Broken/chaotic flux surfaces

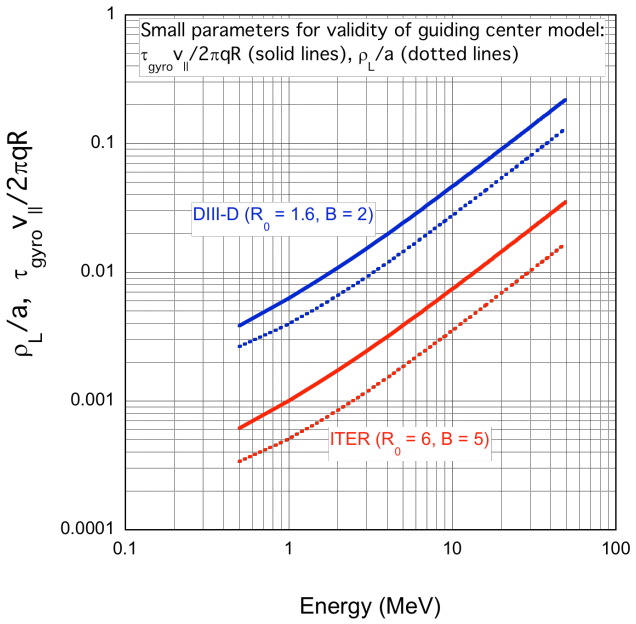

Relativistic orbit trajectory models

Trajectory equations in Boozer Coordinates
[A. Cooper, et al., PPCF **39**, 931 (1997);
R. White, et al., PPPL-5078, 2014]

$$\dot{\theta} = \frac{eB^2\rho_\parallel}{m_0\gamma D}\left(\psi' - \rho_\parallel G'\right) + \frac{G}{\gamma D}\left(\frac{\mu}{e} + \frac{eB\rho_\parallel^2}{m_0}\right)\frac{\partial B}{\partial r}$$

$$\dot{\zeta} = \frac{eB^2\rho_\parallel}{m_0\gamma D}\left(\chi' - \rho_\parallel I'\right) - \frac{I}{\gamma D}\left(\frac{\mu}{e} + \frac{eB\rho_\parallel^2}{m_0}\right)\frac{\partial B}{\partial r}$$

$$\dot{r} = \frac{1}{\gamma D}\left(\frac{\mu}{e} + \frac{eB\rho_\parallel^2}{m_0}\right)\left(I\frac{\partial B}{\partial \zeta} - G\frac{\partial B}{\partial \theta}\right)$$

$$\dot{\rho}_\parallel = -\frac{1}{\gamma D}\left(\frac{\mu}{e} + \frac{eB\rho_\parallel^2}{m_0}\right)\left[\left(\chi' + \rho_\parallel I'\right)\frac{\partial B}{\partial \zeta} + \left(\psi' - \rho_\parallel G'\right)\frac{\partial B}{\partial \theta}\right]$$

where $D = G\chi' + I\psi' + \rho_\parallel\left(GI' - IG'\right)$ $\quad \rho_\parallel = \dfrac{\gamma m_0 \mathrm{v}_\parallel}{eB}$

ψ = poloidal flux, $\quad \chi$ = toroidal flux

$$\gamma = \left(1 - \mathrm{v}^2/\mathrm{c}^2\right)^{-1/2} \qquad \mu = m_0\gamma^2\mathrm{v}_\perp^2/2B$$

+ fluctuating field terms from R. White, et al., PPCF **52** (2010)

Non-canonical coordinates model for following runaways outside closed flux surfaces and including magnetic islands
[J. Cary, A. Brizard, Rev. Mod. Phys. **81**, 693 (2009)]

$$\frac{d\vec{R}}{dt} = \frac{1}{B_\parallel^*}\left(\mathrm{v}_\parallel \vec{B}^* + \vec{E}^* \times \hat{b} + \frac{\mu}{e}\hat{b} \times \vec{\nabla} B\right)$$

$$\frac{d\mathrm{v}_\parallel}{dt} = e\left(\vec{E}^* + \vec{R} \times \vec{B}^*\right)\mu\vec{\nabla} B$$

where $\vec{B}^* = \vec{B} + \dfrac{\gamma m_0 \mathrm{v}_\parallel}{e}\vec{\nabla} \times \hat{b}$ and $\vec{E}^* = \vec{E} + \dfrac{\gamma m_0 \mathrm{v}_\parallel}{e}\dfrac{\partial \hat{b}}{\partial t}$

Magnetic field components in cylindrical geometry based on 3D VMEC ITER model and using Xpand code to extend domain outside last closed flux surface

B_R $\quad B_Z$ $\quad B_\phi$

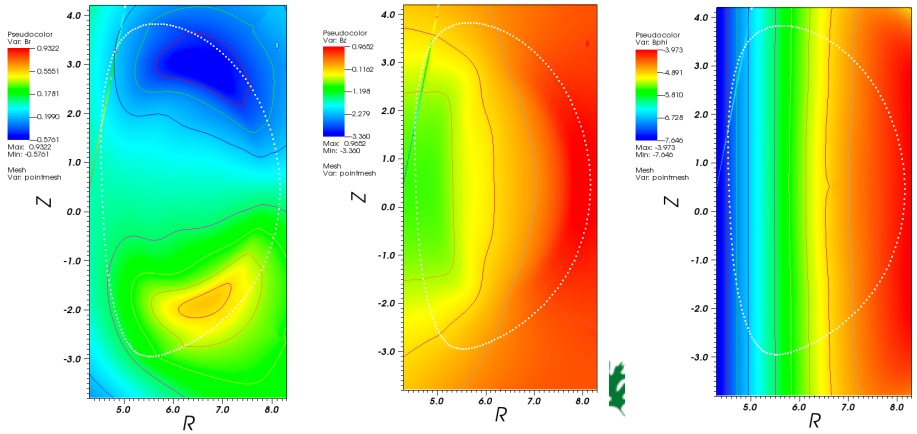

Collision operator model

Collision operator of G. Papp, et al., Nuc. Fusion **51** (2011) 043004, App. B (merges together relativistic and non-relativistic limits for e-e scattering)

$$\lambda = \mathrm{v}_{\parallel}/\mathrm{v} \qquad \mathrm{q} = \gamma \frac{\mathrm{v}}{c} \qquad \gamma = \left(1 - \frac{\mathrm{v}^2}{c^2}\right)^{-1/2}$$

Monte Carlo collision operator:

$$\lambda_{new} = \lambda_{old}\left(1 - \nu_d \Delta t\right) \pm \left[\left(1 - \lambda_{old}^2\right)\nu_d \Delta t\right]^{1/2}$$

$$q_{new} = q_{old} + \nu_{E1}\left(q_{old}\right)\Delta t \pm \left[\nu_{E2}\left(q_{old}\right)\Delta t\right]^{1/2}$$

$$\nu_d = I = \frac{\sqrt{1+q^2}}{\tau q^3}\left[Z_{eff} + \phi(x_e) - G(x_e) + \frac{\varepsilon q^2}{1+q^2}\right]$$

$$\nu_{E1} = \frac{1}{\tau q^2}\left\{-J(q)\left(1+q^2\right) + \frac{\partial}{\partial q}\left[J(q)P(q)\right]\right\}; \quad \nu_{E2} = \frac{1}{\tau q^2}J(q)P(q)$$

$$J(q) = \frac{q^2}{\varepsilon\left(1+q^2\right)}G(x_e); \quad P(q) = \frac{\varepsilon\left(1+q^2\right)^{3/2}}{q}$$

$$\phi(x) = Error\ \ function = \frac{2}{\sqrt{\pi}}\int_0^x e^{-y^2}\,dy; \quad G(x) = \frac{1}{2x^2}\left[\phi(x) - x\phi'(x)\right]$$

$$\varepsilon = \frac{kT_e}{m_e c^2}; \quad x_e = \frac{q}{\sqrt{2\varepsilon\left(1+q^2\right)}}; \quad \tau = \frac{4\pi\varepsilon_0^2 m_e^2 c^3}{ne^4 \ln\Lambda}$$

Collision operator + screened impurity effects

Collision operator of G. Papp, et al., Nuc. Fusion **51** (2011) 043004, App. B (merges together relativistic and non-relativistic limits for e-e scattering)

$$\lambda = v_{\parallel}/v \qquad q = \gamma \frac{v}{c} \qquad \gamma = \left(1 - \frac{v^2}{c^2}\right)^{-1/2}$$

Monte Carlo collision operator:

$$\lambda_{new} = \lambda_{old}\left(1 - \nu_d \Delta t\right) \pm \left[\left(1 - \lambda_{old}^2\right)\nu_d \Delta t\right]^{1/2}$$

$$q_{new} = q_{old} + \nu_{E1}\left(q_{old}\right)\Delta t \pm \left[\nu_{E2}\left(q_{old}\right)\Delta t\right]^{1/2}$$

$$\nu_d = I = \frac{\sqrt{1+q^2}}{\tau q^3}\left[Z_{eff} + \phi(x_e) - G(x_e) + \frac{\varepsilon q^2}{1+q^2}\right]$$

$$\nu_{E1} = \frac{1}{\tau q^2}\left\{-J(q)\left(1+q^2\right) + \frac{\partial}{\partial q}\left[J(q)P(q)\right]\right\} \qquad \nu_{E2} = \frac{1}{\tau q^2} J(q)P(q)$$

$$J(q) = \frac{q^2}{\varepsilon\left(1+q^2\right)} G(x_e); \qquad P(q) = \frac{\varepsilon\left(1+q^2\right)^{3/2}}{q}$$

$$\phi(x) = Error\ \ function = \frac{2}{\sqrt{\pi}} \int_0^x e^{-y^2}\, dy; \quad G(x) = \frac{1}{2x^2}\left[\phi(x) - x\phi'(x)\right]$$

$$\varepsilon = \frac{kT_e}{m_e c^2}; \quad x_e = \frac{q}{\sqrt{2\varepsilon\left(1+q^2\right)}}; \quad \tau = \frac{4\pi\varepsilon_0^2 m_e^2 c^3}{n e^4 \ln\Lambda}$$

Impurity screening effects modify pitch-angle scattering

Impurity screening effects modify slowing-down/drag

L. Hesslow, O. Embréus, et al., PRL **118**, 255001 (2017).

Also, Moscow plasma simulation center report "*Integrated simulation of ITER disruptions and support in development of disruption mitigation systems*"

Modifications to collision frequencies to take into account screening effects

- Fast electron colliding on bound electrons of partially ionized impurities
- Pitch angle scattering: elastic electron-ion collisions
  - Quantum Born approximation, density functional theory
- Energy scattering: inelastic electron-electron collisions
  - Bethe stopping power formula
- We use Hesslow model: equations (4) and (7)

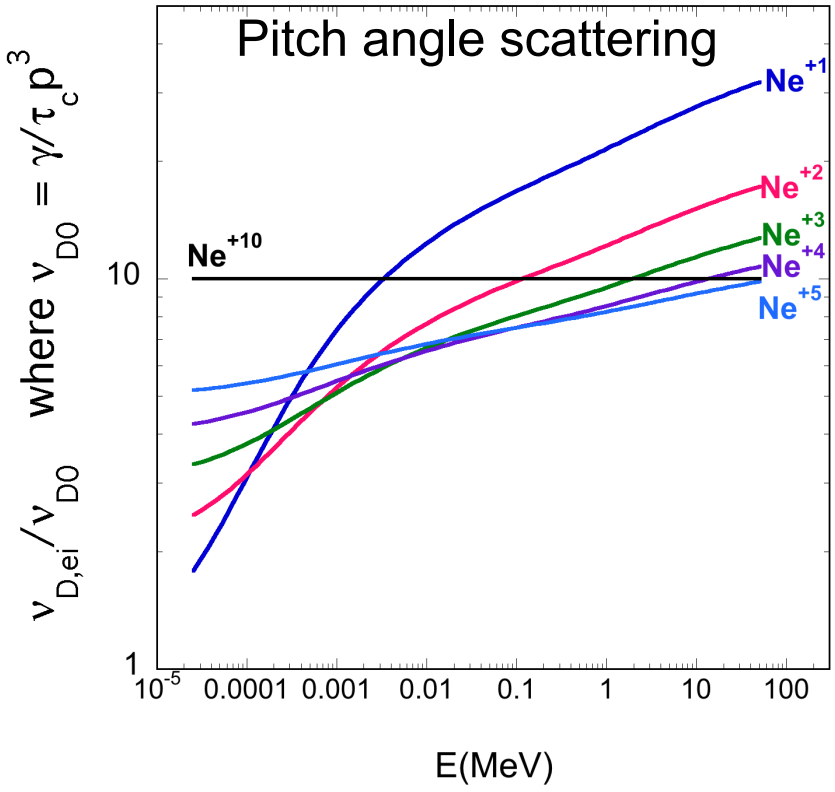

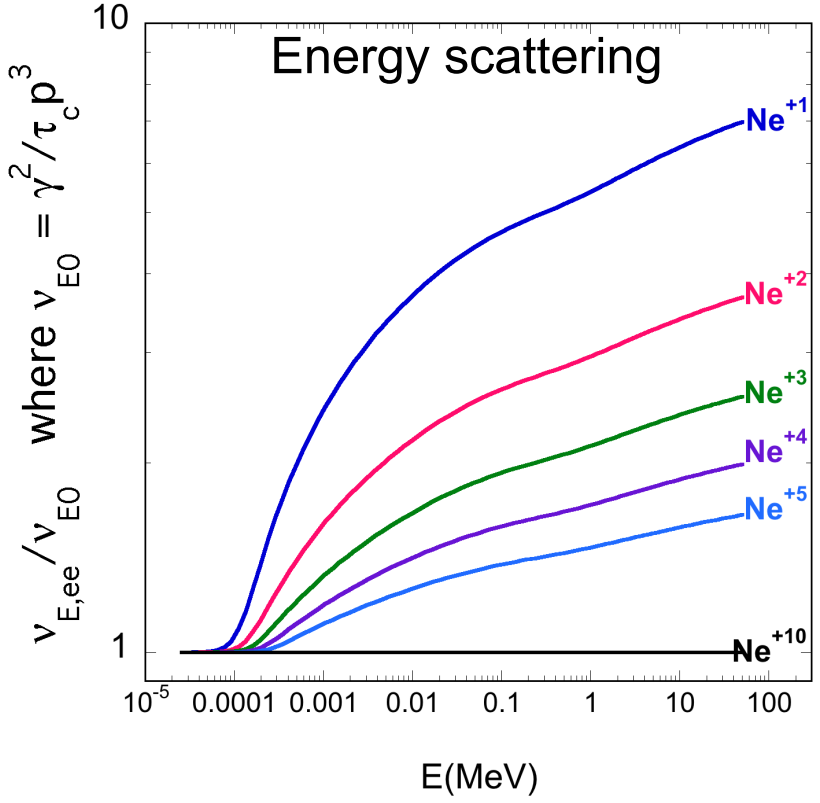

Synchrotron loss model

Synchrotron loss model of G. Papp, et al., Nuc. Fusion 51 (2011) 043004, App. A

$$\frac{d\varepsilon}{dt} = -\frac{\gamma v_\perp^2}{c^2 \tau_r}\varepsilon \quad \text{where} \quad \tau_r = \frac{6\pi\varepsilon_0 (m_0 c)^3}{e^4 B^2}$$

This can be rewritten as:

$$\frac{d\gamma}{dt} = -\frac{\gamma^2 (v_\perp^2 / c^2)}{\tau_r} \Rightarrow \gamma = \gamma_{t=0}\left[1 + \gamma_{t=0}\tau_r^{-1}\int dt (v_\perp^2 / c^2)\right]^{-1}$$

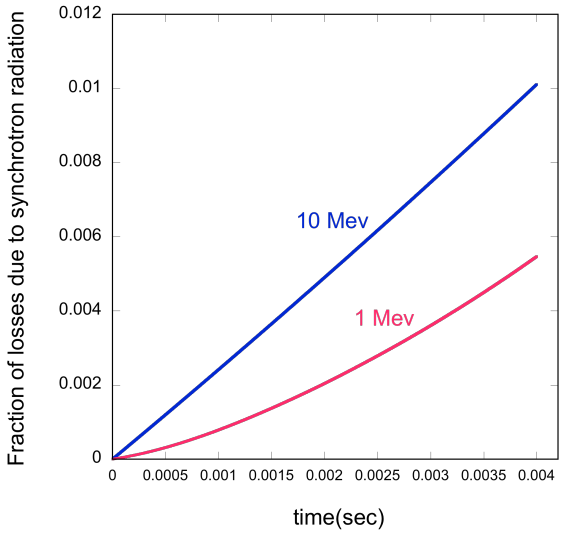

τ_r sets the time scale for synchrotron energy losses
Typically, τ_r is in the range of

- 1.3 seconds for DIII-D parameters
- 0.2 seconds for ITER parameters

Next steps:

- Improved model possible in cylindrical geometry GC model
- More direct incorporation of radiation force
- Comparison/verification with Carbajal's full orbit calculations

Disruption field model/formation/acceleration

- Free-fall acceleration equation

$$\frac{d}{dt}\left(\gamma m_0 \vec{v}\right) = -e\vec{E} = -e\frac{\partial \vec{A}}{\partial t}$$

- Ampere's law

$J_{runaway}$
- Inferred from data
- Runaway generation rates
- Monte Carlo

$$\vec{\nabla}\times\vec{B} = \vec{\nabla}\times\vec{\nabla}\times\vec{A} = \mu_0\vec{J} = \mu_0\left(\vec{J}_{runaway} + \vec{J}_{plasma}\right)$$

- Runaway-dominated limit:

$$\frac{\partial}{\partial R}\frac{1}{R}\frac{\partial}{\partial R}(RA) + \frac{\partial^2 A}{\partial z^2} = \frac{\mu_0 n_{runaway} e^2}{m_0}\frac{A}{\sqrt{1+A^2}} = \frac{k^2 A}{\sqrt{1+A^2}} \quad \text{where} \quad k^2 = \frac{\omega_{pr}^2}{c^2} \quad \text{with} \quad \omega_{pr}^2 = \frac{n_{runaway} e^2}{m_0 \varepsilon_0}$$

k: electron skin depth parameter

where $A \equiv \frac{-e}{m_0 c}\left[A_\phi(\vec{r},t) - A_\phi(\vec{r},t=0)\right]$

$$\frac{v_\phi}{c} = \frac{A}{\sqrt{1+A^2}}$$

Typical disruption current collapse and voltage spike (from L. Baylor, DIII-D case)

$$Current = I_{runaway} = \pi a_r^2 n_{runaway} ec$$

$$\Rightarrow n_{runaway} = \frac{I_{runaway}}{\pi a_r^2 ec}$$

e.g., for estimated paramters of DIII-D runaway dominated case: $I_{runaway} = 300kA, a_r = 25cm$

$$\Rightarrow n_{runaway} = 3.2 \times 10^{10}\, cm^{-3}$$

$$c/\omega_{pe} \approx 3\ cm,\ ka_r = 8.4$$

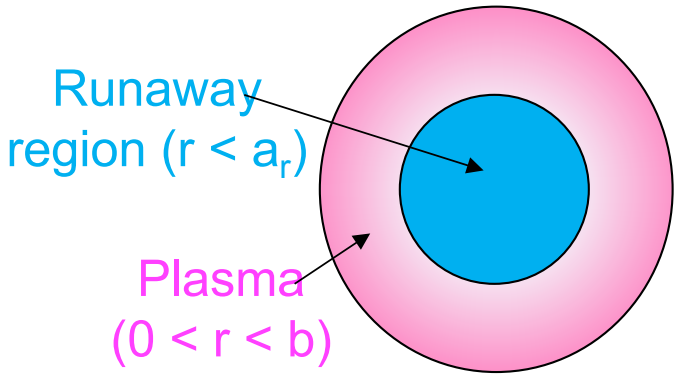

Typical DIII-D current quench => runaway discharge
ΔI = 900 kA, dI/dt ~ - 240MA/sec

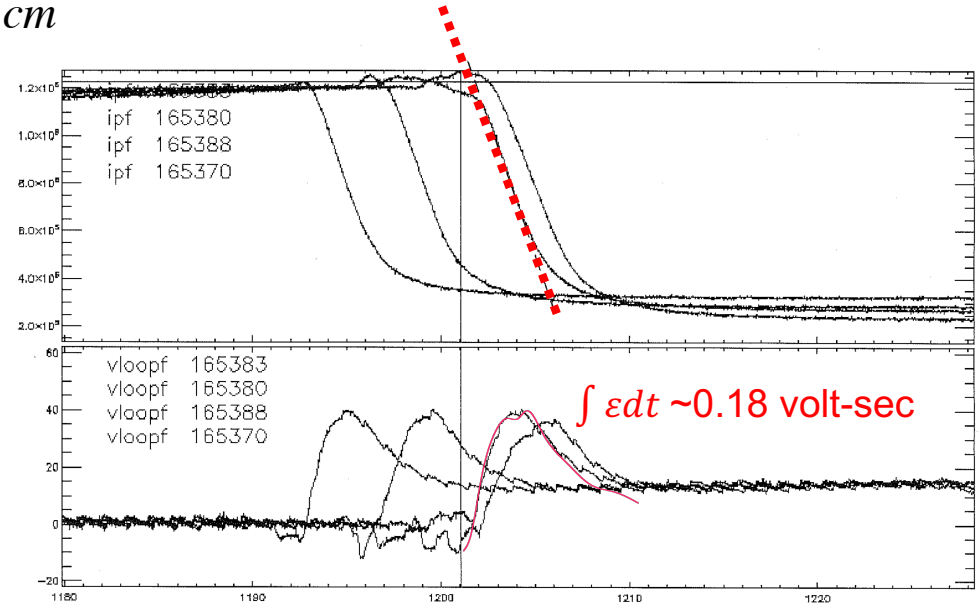

~0.18 v-sec ~1.2 v-sec

$$A(t)\big|_{r=a_r} = \frac{e}{2\pi R_0 m_0 c}\left\{\int_{t_0}^{t} \varepsilon_{loop}(t')dt' - \mu_0 R_0\left[I(t) - I(0)\right]\ln\frac{b}{a_r}\right\}$$

Solving coupled nonlinear acceleration/Ampere's equation indicates:

- Early time acceleration is highly non-uniform
- Runaway current profile fills in with time
- Free-fall limit indicates potential for ~40 Mev electrons from 240 MA/sec quench
- Reduced by collisional effects, losses from disruption stochastic fields, etc.

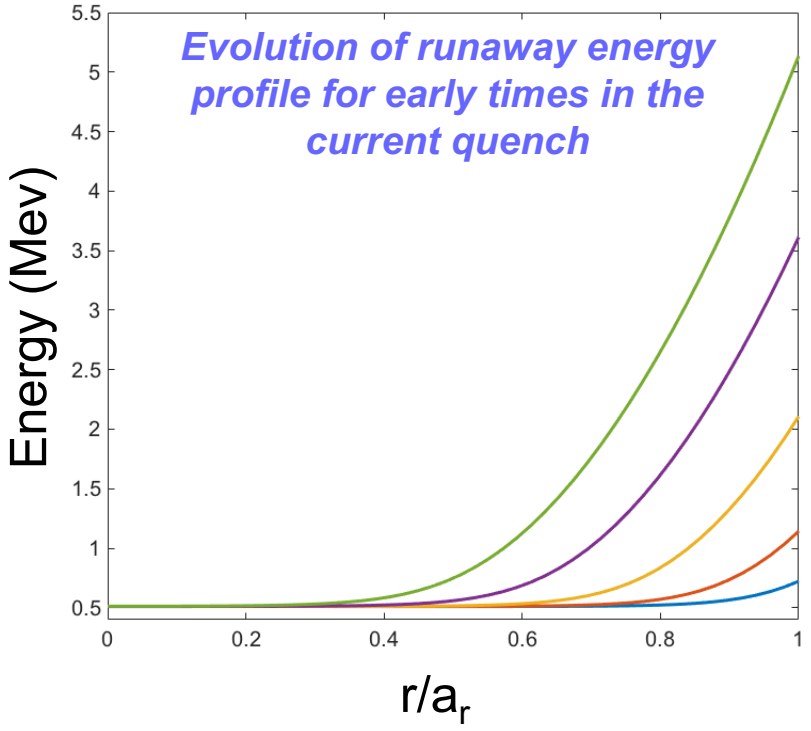

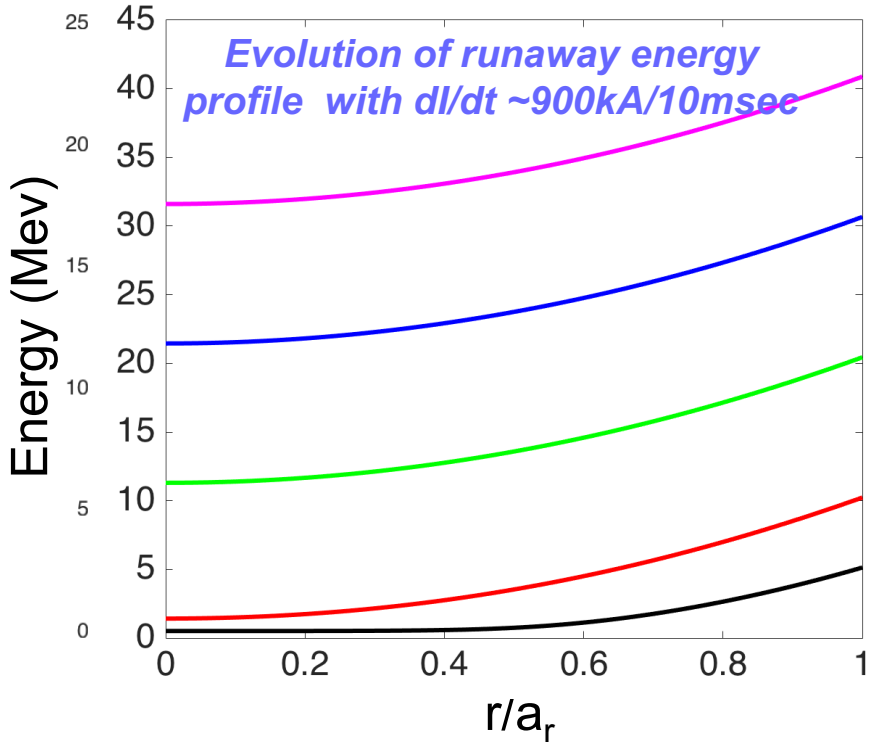

Our modeling is motivated by typical DIII-D current quench, runaway generation, acceleration, suppression cases

[E. Hollmann, Phys. Plasmas 22, 056108 (2015)]

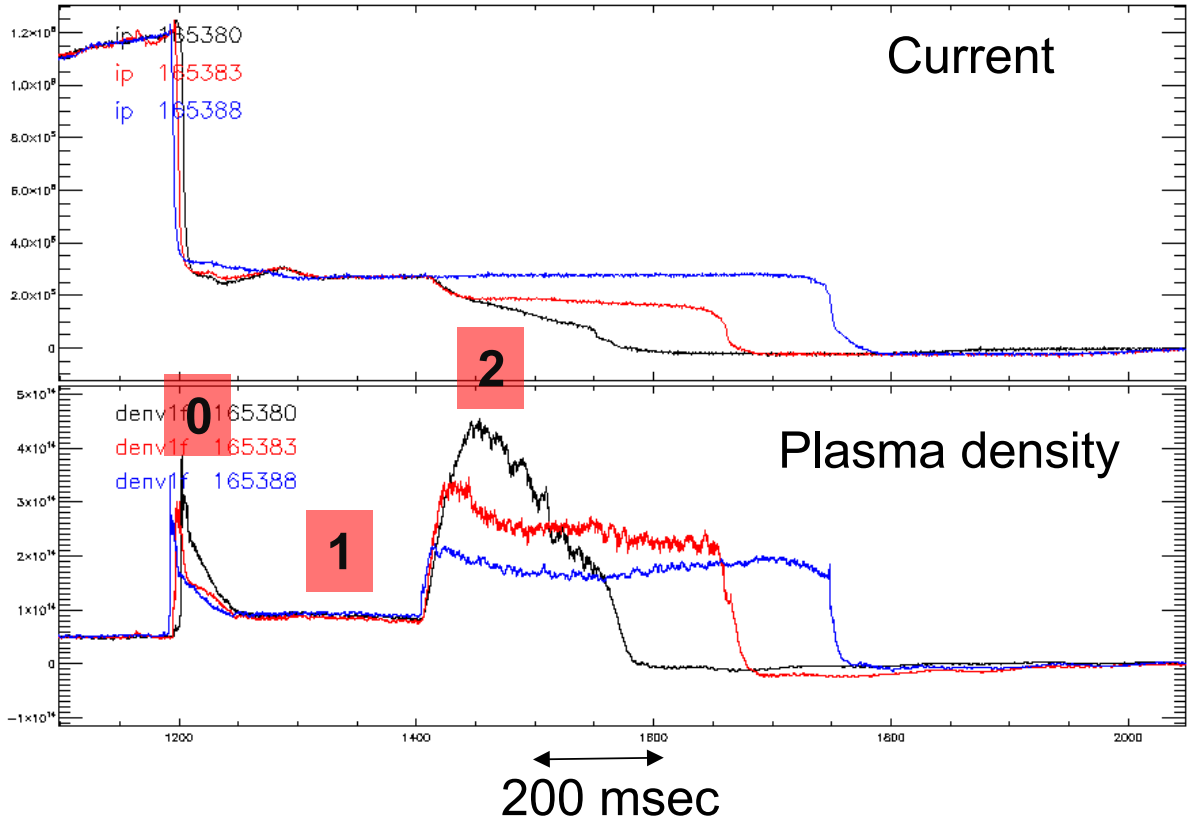

0 1st pellet - current quench: runaway generation

1 Runaway dominated phase
Z_{eff} = 12, $n_e(0)$ = 2 x 10^{14} cm^{-3}
$T_{ion}(0) = T_{elec}(0)$ = 2 eV

2 Neon pellet: runaway suppression
Z_{eff} = 10, $n_e(0)$ = 1 x 10^{15} cm^{-3}
$T_{ion}(0) = T_{elec}(0)$ = 2 eV

Modeling of pellet-induced current dissipation phase

Averaged over ensemble of 15,360 runway orbits

Followed with Monte Carlo collisions for up to 100 msec

Initial conditions: $v_{||}/v = 0.9$

Hollow runaway density localized to $\psi_0/\psi_{edge} = 0.2$

Initial runaway energy varied: 0.5 Mev to 20 Mev

0 Current quench: generates runaways

1 Before pellet:
$Z_{eff} = 10$,
$n_e(0) = 2 \times 10^{14}$ cm^{-3}
$T_{ion}(0) = T_{elec}(0) = 2$ eV

2 After neon pellet:
$Z_{eff} = 12$
$n_e(0) = 1 \times 10^{15}$ cm^{-3}
$T_{ion}(0) = T_{elec}(0) = 2$ eV

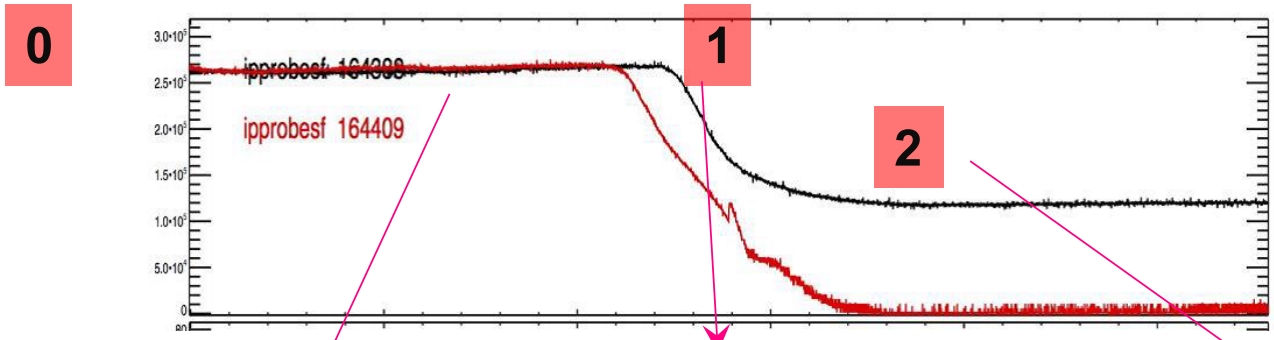

Gradual energy loss phase

More rapid energy loss

Rapid runaway current decay

Sensitivity of decay rates to initial runaway energy

- Runaways initialized at 5,10, 15, 20 MeV
- Plasma ions consist of fully ionized impurity: Ne^{+10} only
- $n_e=10^{15}$ cm^{-3}, T_e = 2 eV, Z_{eff} = 10

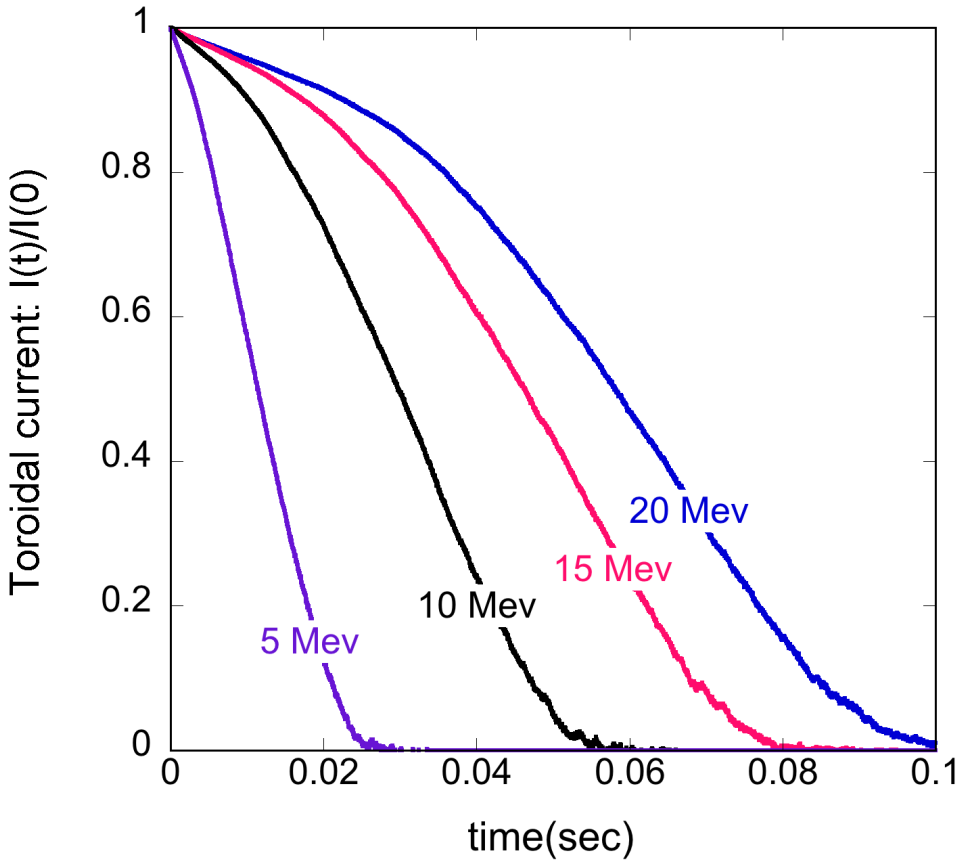

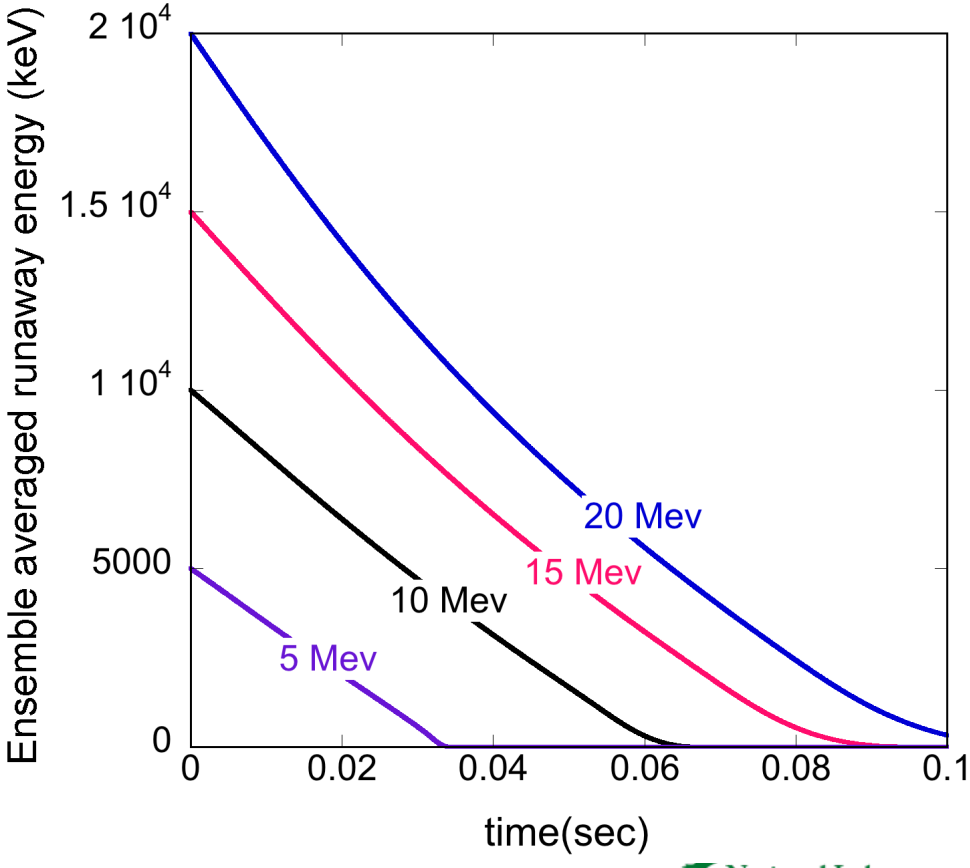

Sensitivity of decay rates to plasma density

- Initial runaways at 10 MeV, T_e = 2 eV, Z_{eff} = 10
- Plasma ions consist of fully ionized impurity: Ne^{+10} only
- n_e=10^{14} cm^{-3}, 2 x 10^{14} cm^{-3}, 5 x 10^{14} cm^{-3}, 10^{15} cm^{-3}

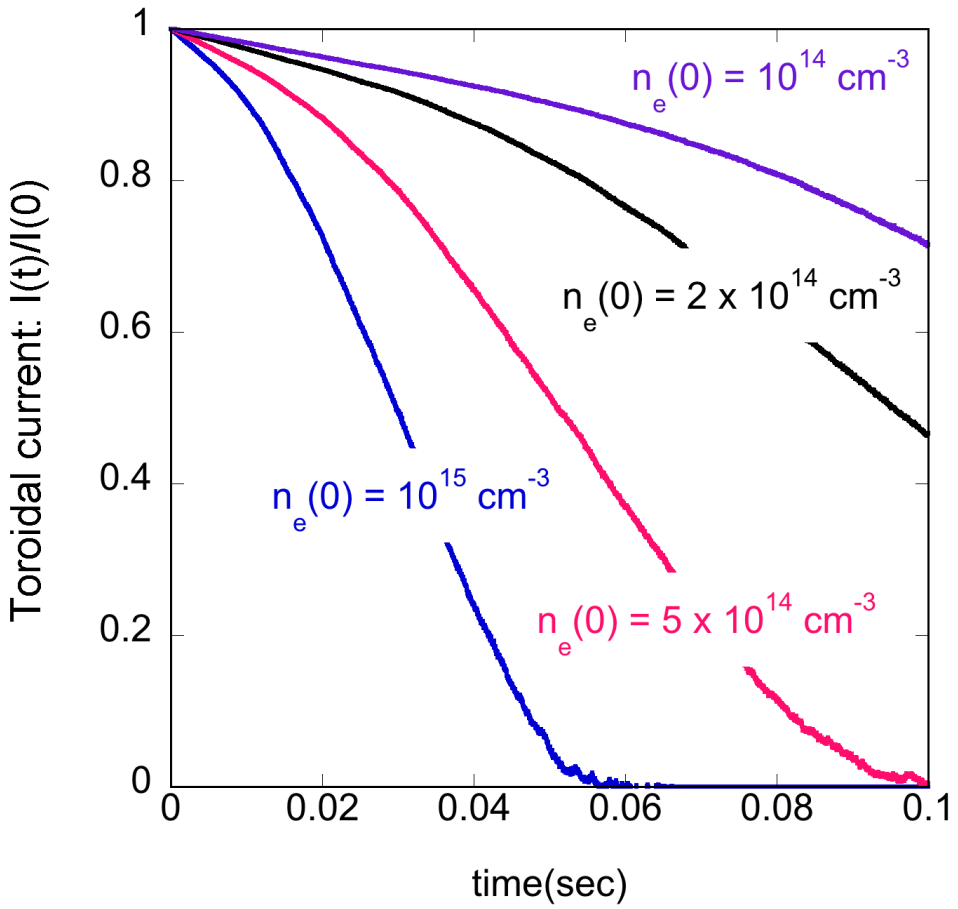

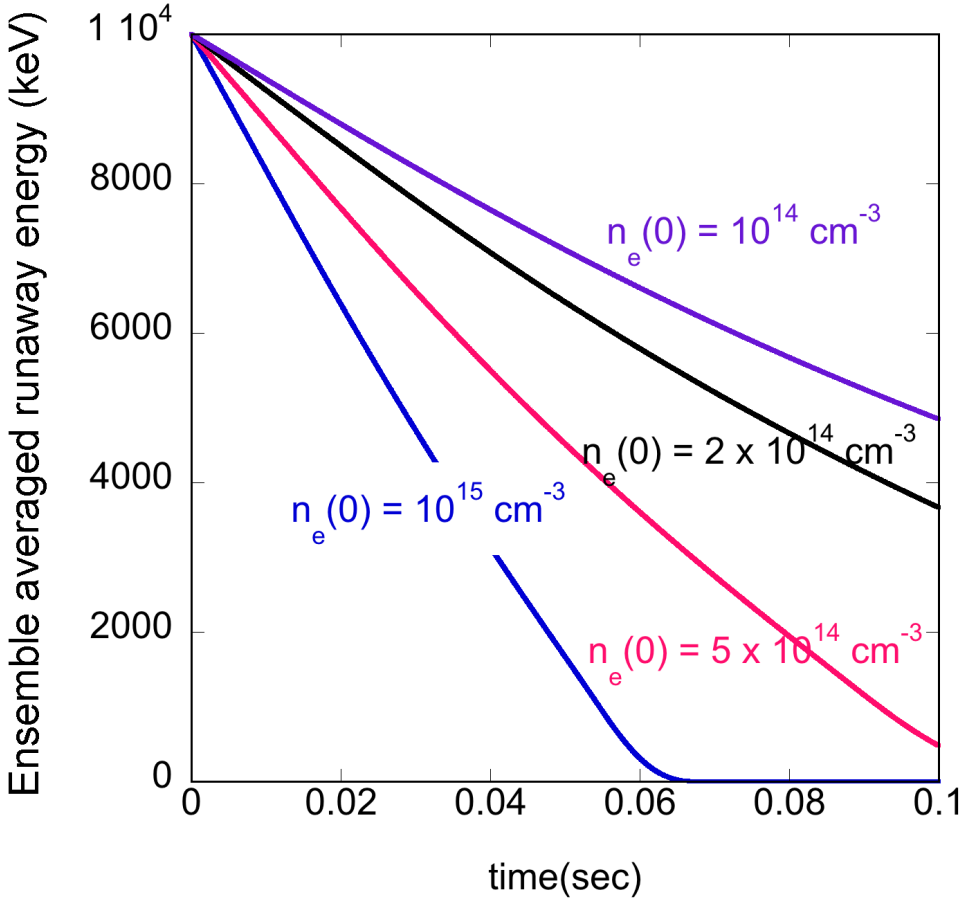

Sensitivity of decay rates to plasma electron temperature

- Initial runaways at 10 MeV, $n_e = 10^{14}$ cm^{-3}, $Z_{eff} = 10$
- Plasma ions consist of fully ionized impurity: Ne^{+10} only
- T_e = 100 eV, 500 eV, 1 keV

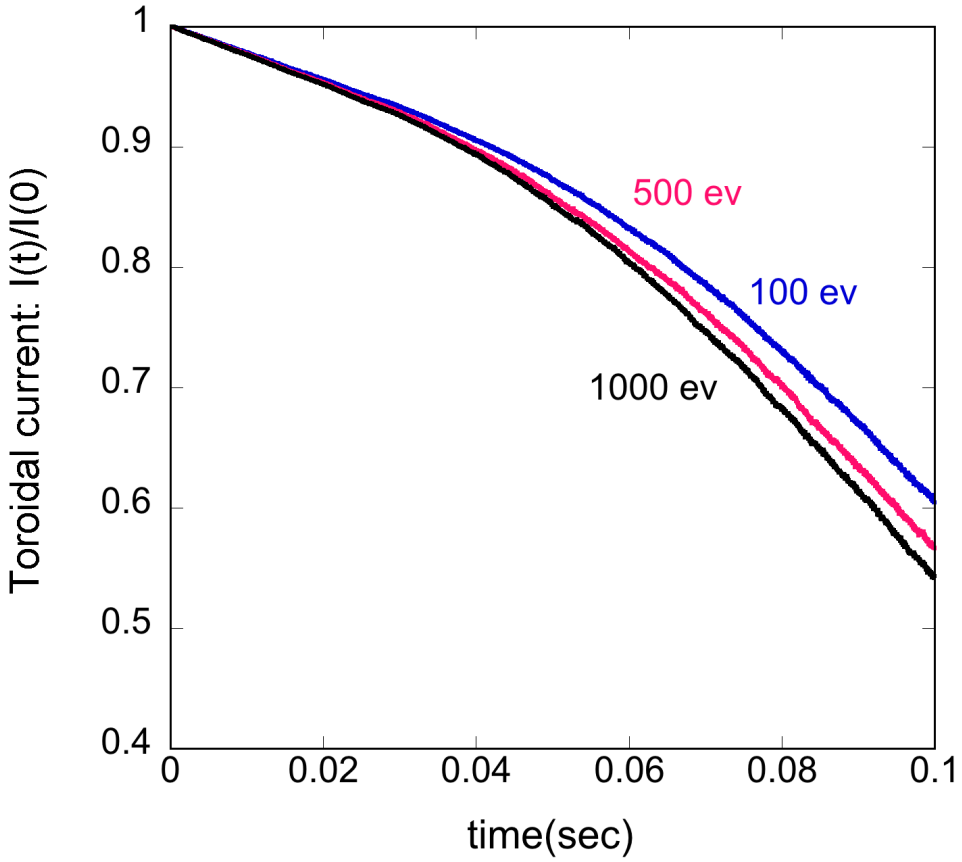

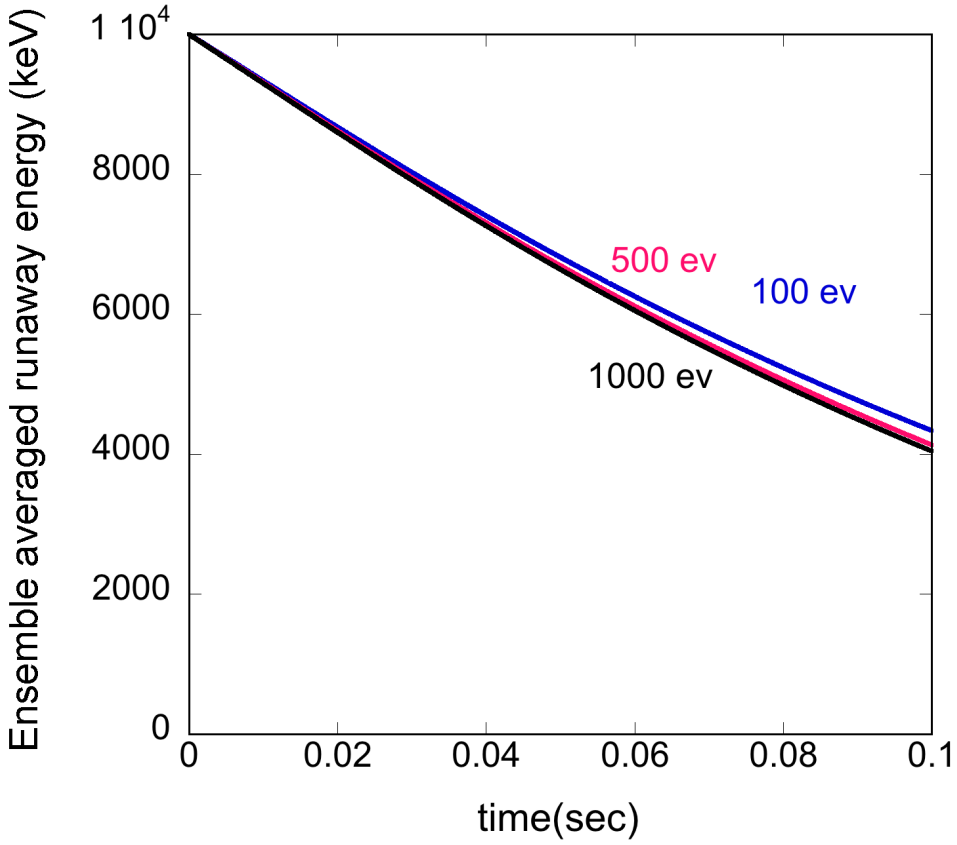

Impurity charge state has strong effect on current and energy decay rate

- Initial runaways at 10 MeV, $n_e=10^{15}$ cm^{-3}
- Ne^{+10} = fully ionized; Ne^{+1}, Ne^{+2}, Ne^{+5} = partially ionized states
- Ne^{+1} provides strongest suppression effect

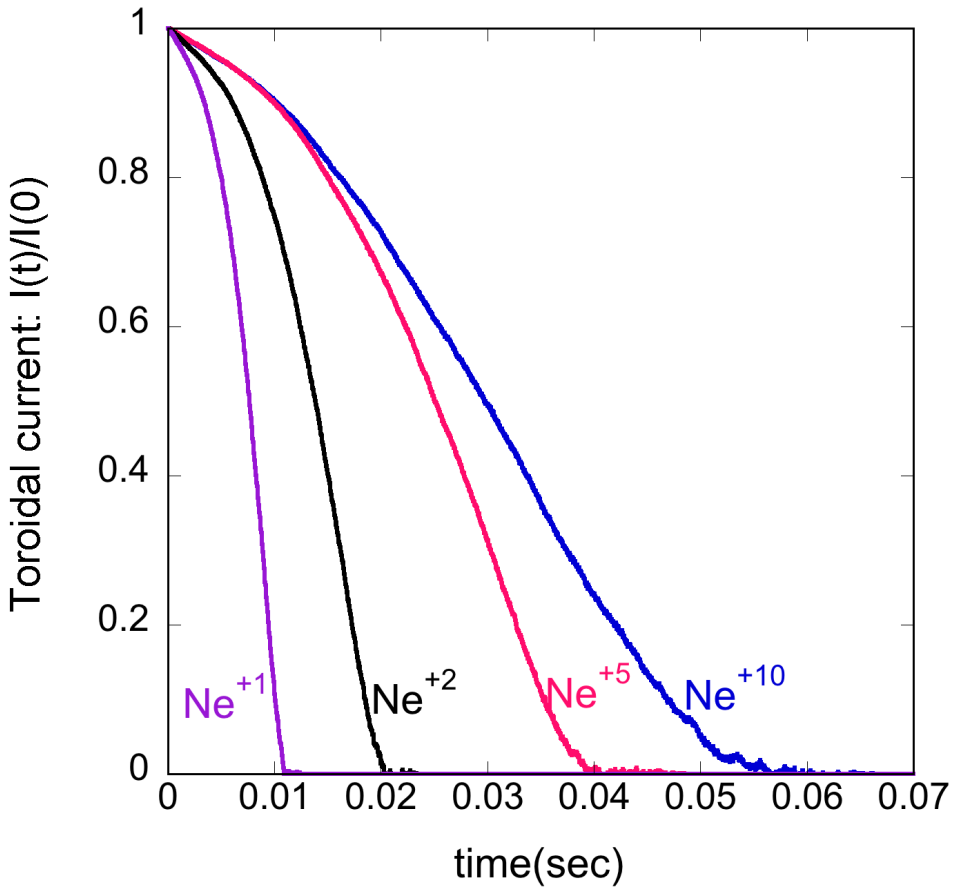

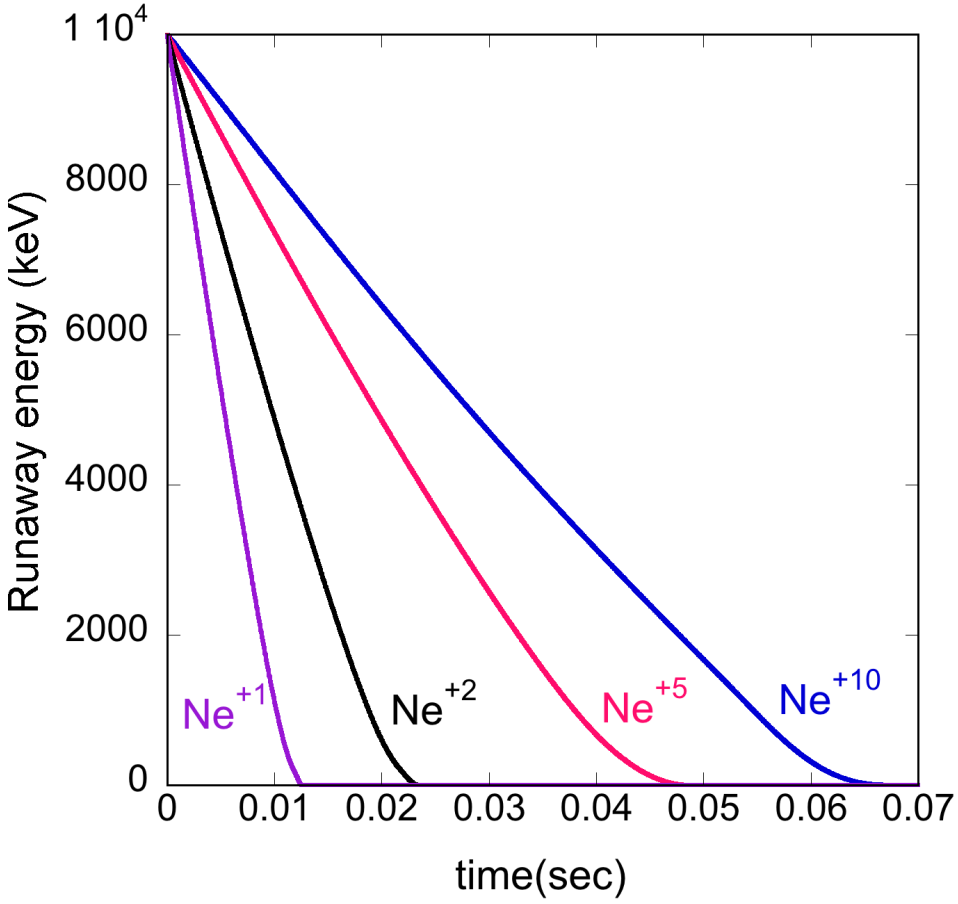

Runaway density distribution spreads with time from effect of collisions

- More spreading at higher collisionalities
  - lower runaway energy
  - Higher plasma density

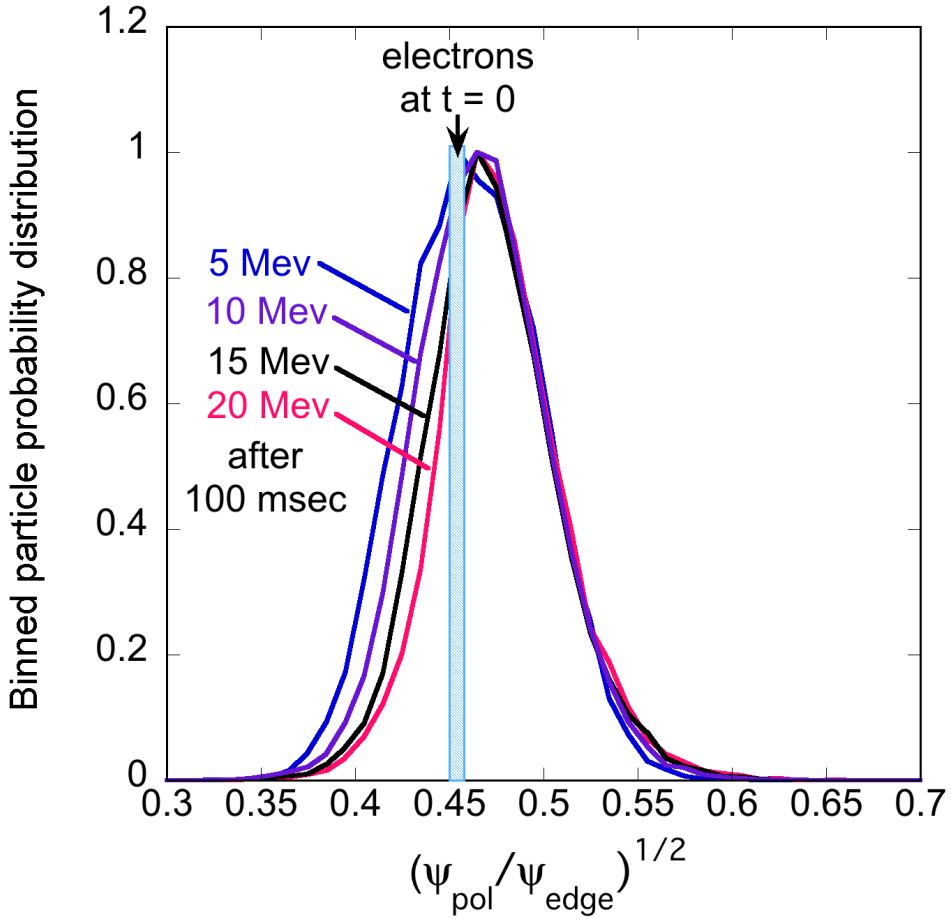

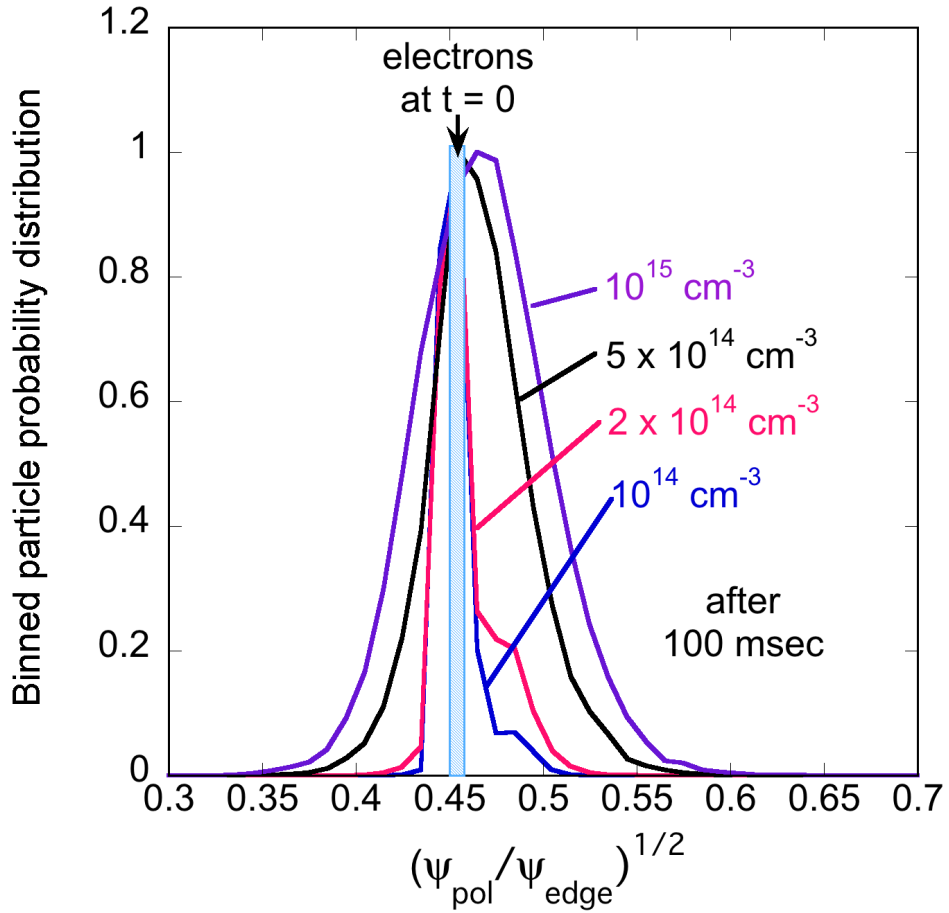

But variation with degree of charge screening is exception to this behavior

- Lower charge states (more screening) have higher collisionality, but less spread
- Much faster slowing-down of the runaways for lower charge states allows less time for transport

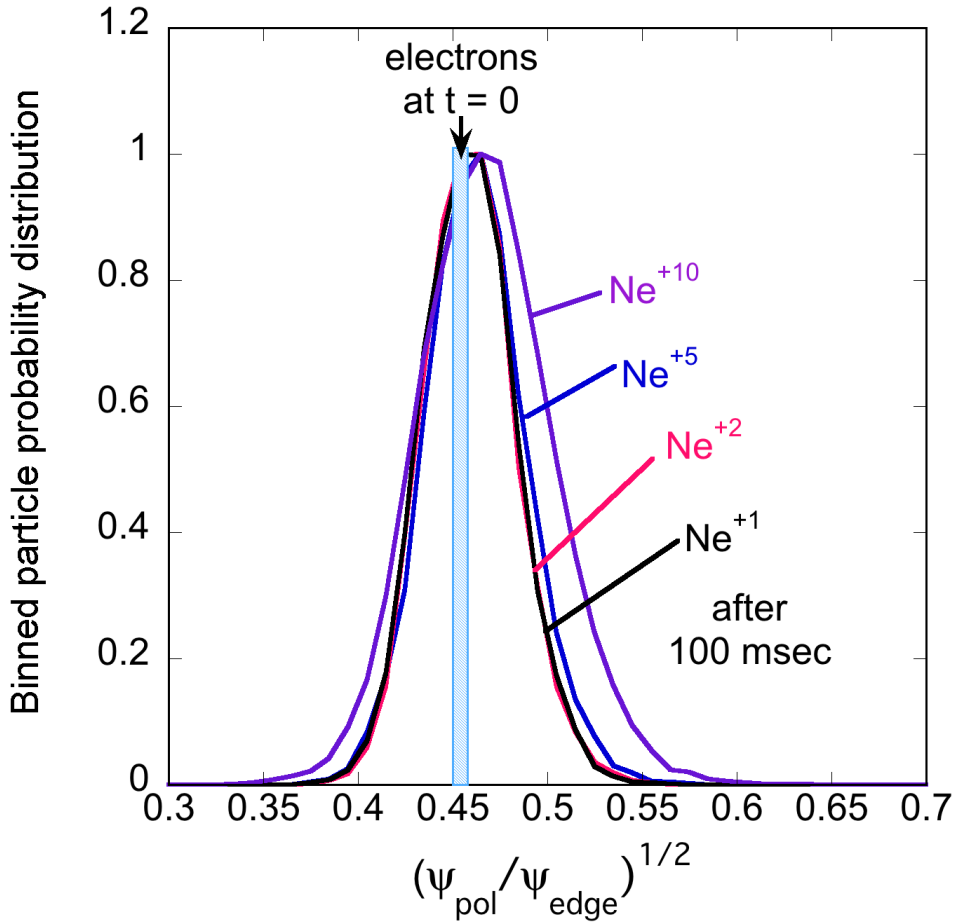

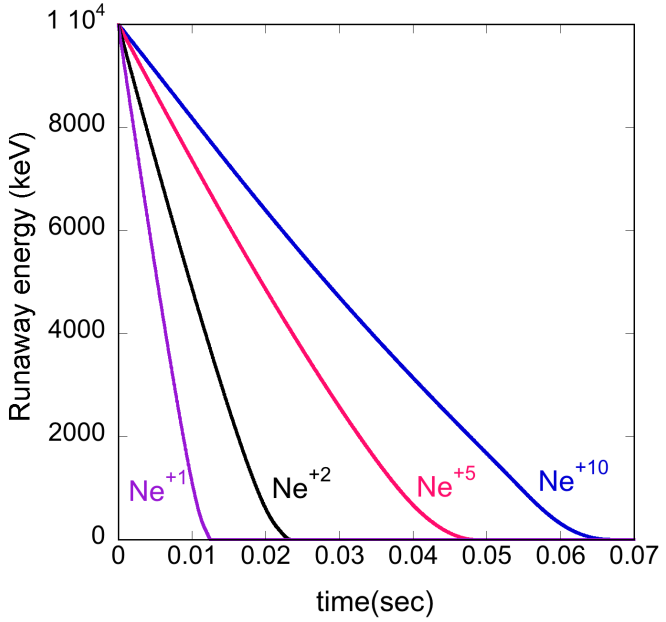

Summary of Monte Carlo runaway dissipation analysis

- Simulation energies/times are up to 20 MeV and 100 msec
- Sensitivity studies made of current and energy decay with pellet induced density and impurity changes
  - Current decay rates bracket experimental observations
- Runaways remain confined with Gaussian spread in density about initial surface.
- Partially stripped impurity collisions recently implemented using model of L. Hesslow, O. Embréus, et al., PRL **118**, 255001 (2017).
- Future directions
  - Include energy/pitch angle distributions, radial profiles, electric field
  - Applications to ITER
  - Cylindrical geometry + follow orbits outside LCF
  - Include model of stochastic disruption fields
  - Knock-on runaways, Bremmstrahlung
  - RMP fields, ripple, MHD mode structures

Runaway interactions with waves

- MHD instabilities
  - Islands, chaotic field lines, 3D fields
- Alfvén instabilities
  - Non-resonant scattering
  - Long residence of runaways in presence of wave coupled with random Coulomb collisions
- Whistler instabilities
  - Coupling through resonances (Anomalous Doppler, Cherenkov)
  - Driven by anisotropy, radial gradients, non-monotonic f(E)
- Whistler/Alfvén activity was topic of recent DIII-D Frontier Science experiment for which I was session leader
  - Connections to ionospheric/solar/astro-physics

Alfvén fluctuations and runaway electrons

- Alfvén waves generally present in all tokamak regimes
- Can be excited by beams/ICRF/hot electrons/alpha particles
- ITER: alphas can survive thermal collapse and drive AE's (?)

Alfvén modes predicted by TAEFL model for DIII-D runaway discharge

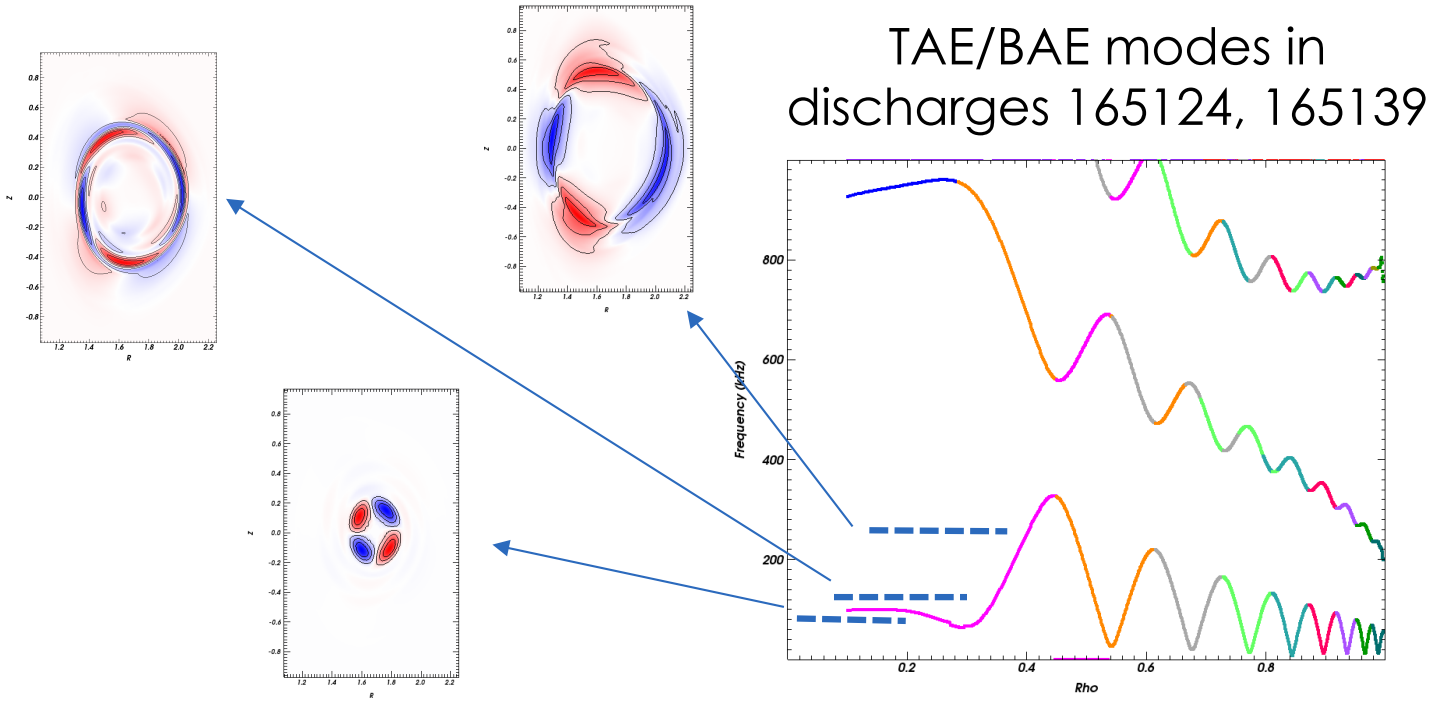

AE mode accelerates current decay – due to enhanced pitch angle scattering

- Initial runaways at 10 MeV, $n_e=10^{15}$ cm^{-3}
- Ne^{+5} = partially ionized impurity

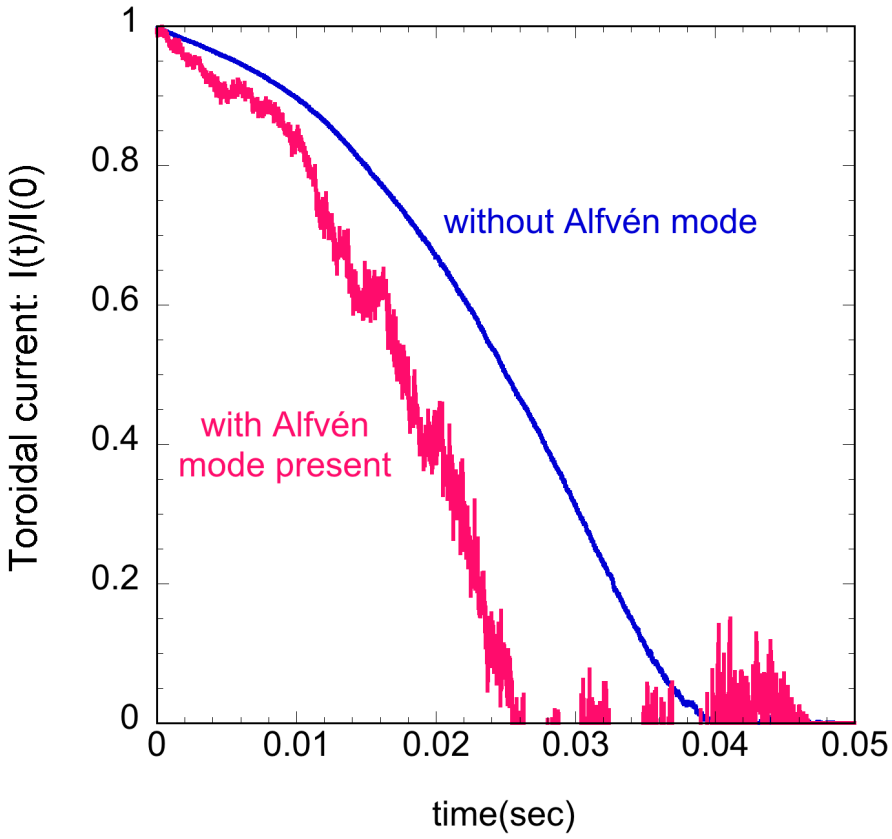

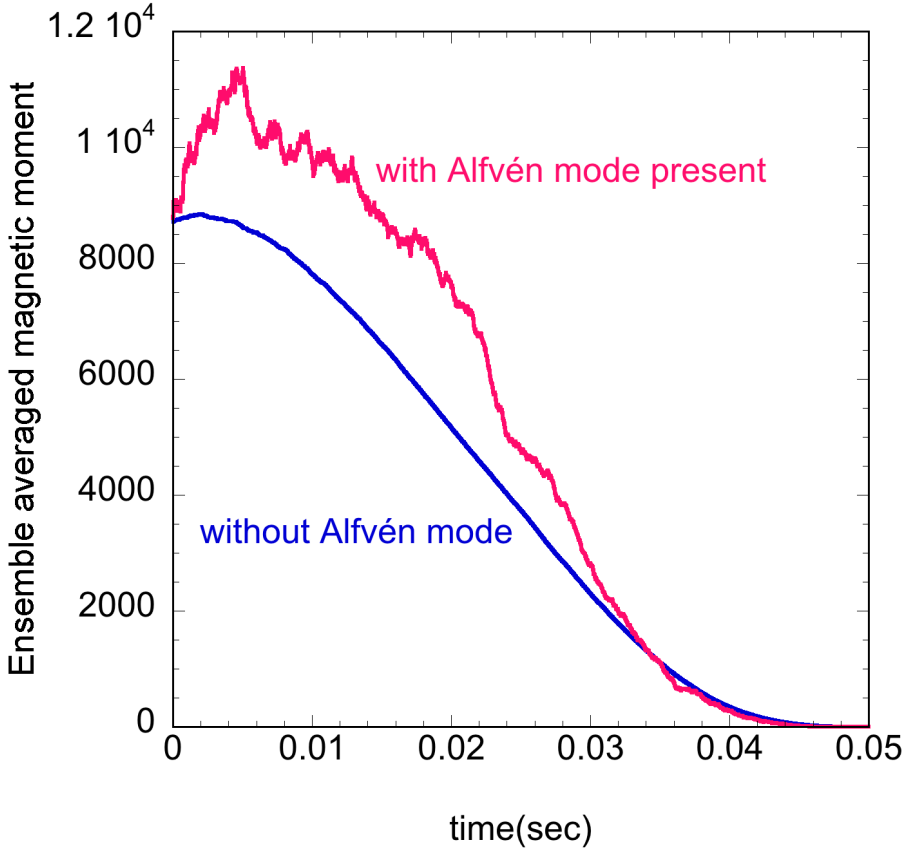

DIII-D runaway/whistler May 31, 2017 experiments - Frontier Science Program

D. A. Spong, W. Heidbrink, C. Paz-Soldan, X.D. Du, K. Thome, M.V. Zeeland, C. Collins, R. Moyer, A. Lvovskiy
+ outside collaborators C. Liu, D. Brennan, T. Fülöp

- B_t = 1 to 1.9 T, density = 0.7 to 1 x 10^{19} m^{-3}
- Frequencies measured using outboard/edge magnetic loop in the 100 to 200 MHz range
- For B_t = 1, n = 1 x 10^{19} m^{-3}
  - f_{ce} = 28 GHz, f_{ci} = 7.6 Mhz
    f_{pe} = 28.4 GHz, f_{lh} = 461 MHz
- Frequencies measured in the ranges
  - 13 f_{ci} < f < 26 f_{ci}
  - 0.0036f_{ce} < f < 0.0071f_{ce}

First detailed measurements of whistler fluctuations in a tokamak (DIII-D)

- 100 to 200 MHz activity correlated with runaway intensity
- Frequency spectra measured with external straps/antennas
  - Follows whistler dispersion relation, quantized into discrete lines
- Intermittent characteristics
  - Whistler waves scatter medium energy runaways in pitch angle (ECE)
  - Less direct effect on high energy runaways (hard x-ray)
  - Sawtoothing - affects runaways near q = 1

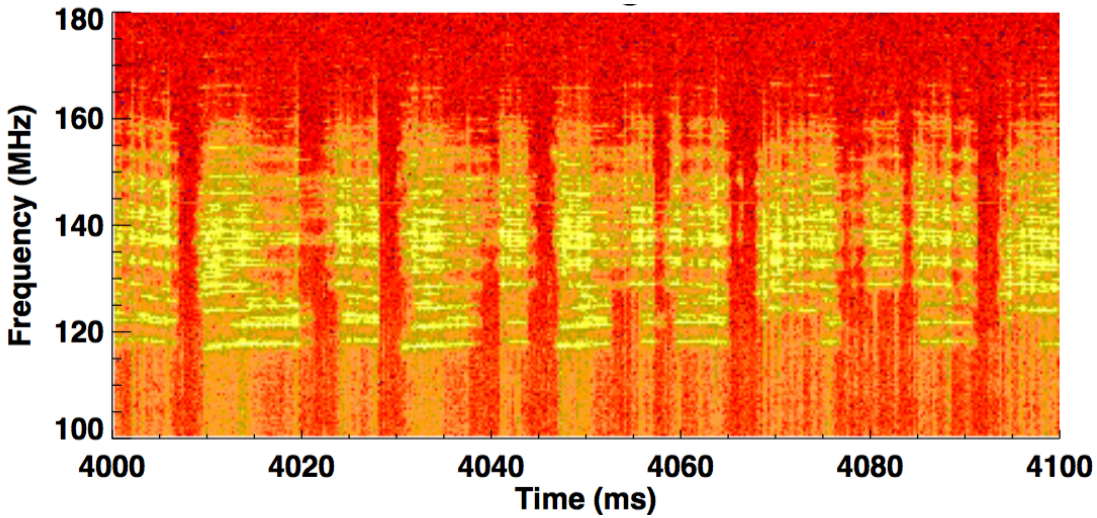

A first look at toroidal geometry/periodic mode structure effects that may explain the multiple frequency bands

Toroidal mode n = 10 MHD continua
poloidal modes m = 0 to 120

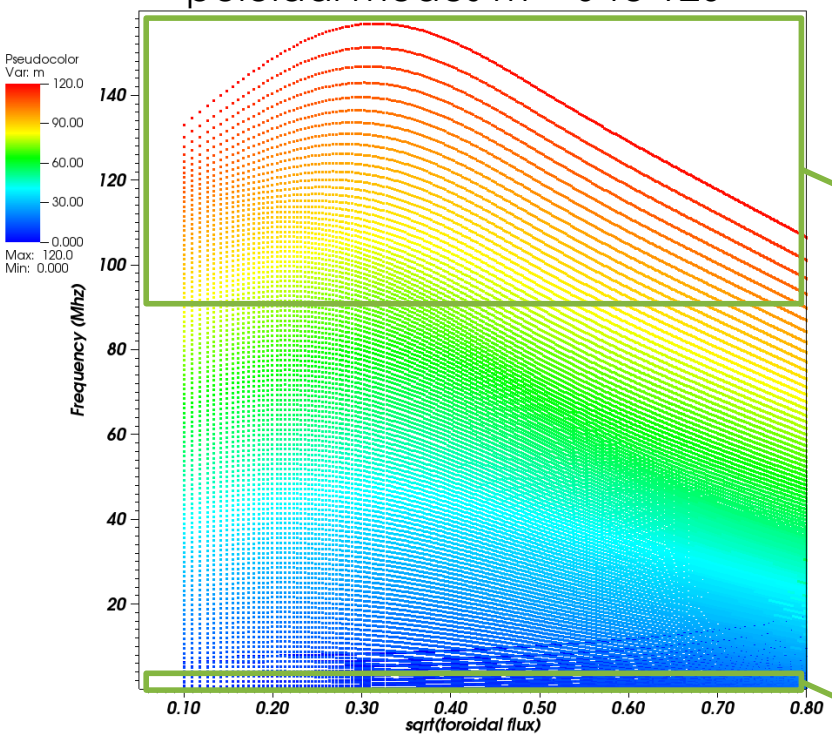

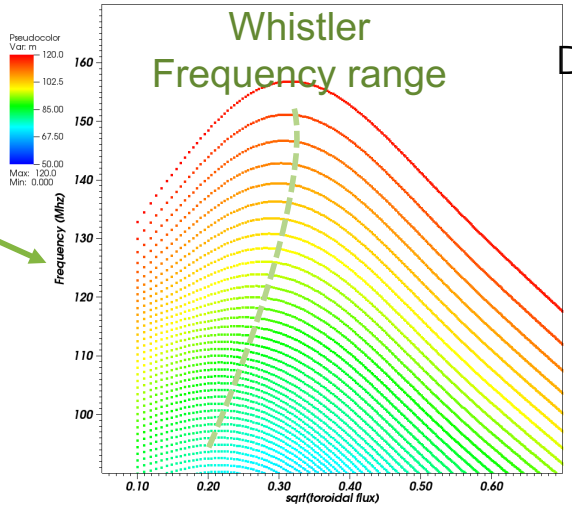

Discrete global modes exist above maxima in these curves (extremal modes)

maxima near axis
r/a ~0.2 to 0.35

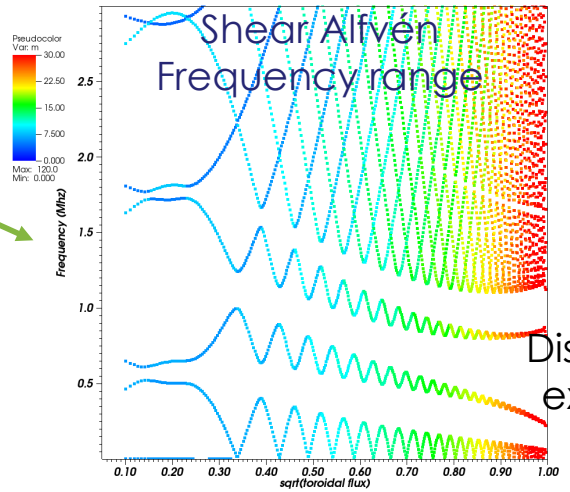

Discrete global modes exist in gap locations

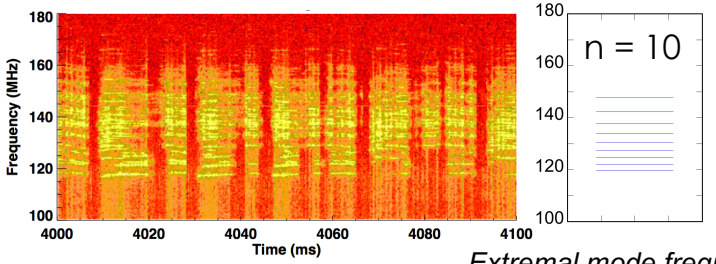

Extremal mode frequencies

Conclusions

- **Monte Carlo modeling of runaway electron suppression by shattered pellets demonstrated**
  - Linearized Coulomb collisions + synchrotron radiation losses
  - Pellet injection causes current/energy decay
  - Modeling in similar regime as DIII-D pellet experiments
  - Partially stripped impurity component can have a strong runaway suppression effect
  - Additional physics to be added (runaway profile effects, time varying plasma parameters, ITER cases, islands, knock-on runaways, etc.)
- **Wave effects and runaways – new control methods**
  - Alfvén modes can cause non-resonant cumulative scattering
  - Whistler modes observed in DIII-D Frontier Science expt.
    - Scatter medium energy runaways
    - Correlated with runaway intensity
    - Discrete frequency bands in the 100 – 200 kHz range